KINETIC TRANSPORT MODEL FOR CELLULAR REGULATION OF pH AND SOLUTE CONCENTRATION IN THE RENAL PROXIMAL TUBULE

A. S. VERKMAN AND ROBERT J. ALPERN
Department of Medicine and Division of Nephrology, Cardiovascular Research Institute, University of California, San Francisco, California 94143

ABSTRACT An open circuit kinetic model was developed to calculate the time course of proximal tubule cell pH, solute concentrations, and volume in response to induced perturbations in luminal or peritubular fluid composition. Solute fluxes were calculated from electrokinetic equations containing terms for known carrier saturabilities, allosteric dependences, and ion coupling ratios. Apical and basolateral membrane potentials were determined iteratively from the requirements of cell electroneutrality and equal opposing transcellular and paracellular currents. The model converged to membrane potentials accurate to 0.05% in one to four iterations. Model variables included cell concentrations of Na, K, HCO_3, glucose, pH (uniform CO_2), volume, and apical and basolateral membrane potentials. The basic model contained passive apical membrane transport of Na/H, Na/glucose, H and K, basolateral transport of $Na/3HCO_3$, K, H, and glucose, and paracellular transport of Na, K, Cl, and HCO_3; apical H and basolateral 3Na/2K-ATPases were present. Apical Na/H and basolateral K transport were regulated allosterically by pH. Apical Na/H transport, basolateral $Na/3HCO_3$ transport, and the 3Na/2K-ATPase were saturable. Model parameters were chosen from data in the rat proximal tubule. Model predictions for the magnitude and time course of cell pH, Na, and membrane potential in response to rapid changes in apical and peritubular Na and HCO_3 were in excellent agreement with experiment. In addition, the model requires that there exist an apical H-ATPase, basolateral $Na/3HCO_3$ transport saturable with HCO_3, and electroneutral basolateral K transport.

INTRODUCTION

The mammalian proximal tubule is a leaky epithelium of one cell type that is responsible for reabsorption of the majority of Na, Cl, HCO_3, glucose, amino acids, and H_2O filtered by the glomerulus. The fluxes of NaCl and $NaHCO_3$ are precisely regulated for normal whole organism acid–base balance and volume homeostasis. Transcellular H_2O and solute movement across the luminal membrane, cell cytoplasm, and basolateral membrane are driven by a basolateral 3Na/2K-ATPase. The highest electrical conductance across the proximal tubule epithelium is across the paracellular pathway (Fromter, 1982).

A number of recent experimental studies in intact tubules and isolated membrane vesicles have extended our knowledge of the transport characteristics of the apical and basolateral membranes in the mammalian proximal tubule (Fig. 1). The apical membrane contains an electroneutral Na/H countertransporter that is saturable in Na and H and regulated allosterically by intracellular pH (Aronson et al., 1982, 1983). There are electrogenic, Na-coupled glucose and amino acid transporters on the apical membrane (Fromter, 1984), and small conductances for H and K (Fromter, 1984; Verkman and Ives, 1986*a*). There is probably an H-ATPase (Kinne-Saffran et al., 1982). The pathways for apical membrane Cl transport are less well-defined; there may be electroneutral $Cl/OH(HCO_3)$ countertransport or Na/Cl cotransport (Warnock and Eveloff, 1982).

Several laboratories have recently identified a basolateral electrogenic $Na/3HCO_3$ cotransporter with a 1:3 Na to HCO_3 coupling ratio saturable in sodium and bicarbonate (Alpern, 1985; Biagi, 1985; Boron and Boulpaep, 1983; Akiba et al., 1986; Grassl and Aronson, 1986; Sasaki et al., 1986; Yoshitomi et al., 1985). There is a small basolateral H conductance, a K conductance (Burckhardt et al., 1984*a*) regulated allosterically by pH (Biagi and Sohtell, 1986), and electroneutral glucose and amino acid exit pathways (Fromter, 1979). The 3Na/2K-ATPase has a 3:2 coupling ratio and is saturable with cell Na and peritubular K (Jorgensen, 1980). Recent experiments suggest that basolateral Cl exit pathways are neutral and coupled to K or to Na and HCO_3 (Guggino et al., 1982; Guggino et al., 1983; Shindo and Spring, 1981; Cassola et

Address offprints requests to Dr. Verkman at 1065 Health Sciences East Tower, University of California, San Francisco, CA 94143.

Dr. Alpern's present address is Department of Internal Medicine, University of Texas Health Sciences Center, 5323 Harry Hines Blvd., Dallas, TX 75235.

BIOPHYS. J. © Biophysical Society · 0006-3495/87/04/533/14 $1.00
Volume 51 April 1987 533–546

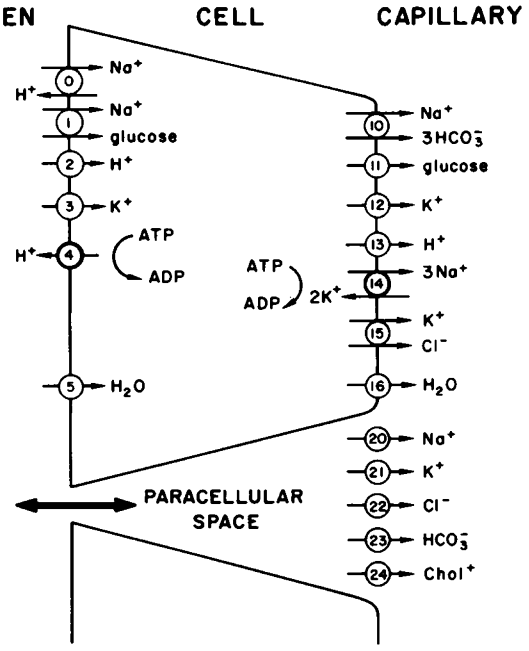

FIGURE 1 Schematic of proximal tubule cell transport. All transporters are numbered. Solute and H_2O flux is generally defined as positive in the resorptive direction (lumen to capillary).

al., 1983; Burckhardt et al., 1984*a*; Eveloff et al., 1985; Illsley et al., 1986).

Based on these known characteristics of proximal tubule transport, we developed a mathematical model to calculate the time course of proximal tubule cell pH, solute concentrations, and membrane potentials in response to acute perturbations in apical or peritubular fluid composition. Previous nonequilibrium thermodynamic models of the proximal tubule assumed linear dependences of solute flows on electrochemical driving forces (Weinstein, 1983); the present model specifically includes known nonlinear effects of transporter saturabilities and allosteric dependences. Model parameters were selected from the literature of the mammalian proximal convoluted tubule; data from the rat were used where available. The model was tested using data from electrophysiological studies and from in vivo fluorescence experiments, where the time course of cellular pH was measured after rapid changes in apical and peritubular fluid composition. Model calculations led to both expected and unexpected effects.

GLOSSARY

Symbols and Definitions

$[X]$	Cell activity of solute X (mM)
$[X]_1$	Luminal activity of solute X (mM)
$[X]_2$	Peritubular activity of solute X (mM)
a_X	Cell activity coefficient of solute X
ϕ_X	Osmotic coefficient of solute X
V	Cell volume (nl)
V_0	Cell volume per millimeter tubule length (nl/mm)
B(pH)	Cell buffer capacity (mmol/mm · pH unit)
J_i	Turnover rate of ith transporter (Fig. 1). For a solute X, the magnitude of solute flux (J^{X_i}, pmol/mm · min) is equal to J_i multiplied by the number of X molecules transported per turnover event. For water, the units for J_i are nl/mm · min. Positive solute and water flux is defined by the direction of the arrows in Fig. 1.
I_1	Lumen to cell membrane current (peq/mm · min)
I_2	Cell to capillary membrane current (peq/mm · min)
I_t	Lumen to capillary paracellular current (peq/mm · min)
P_i	Permeability coefficient (or pump rate) for ith transporter; units given in Table I.
K_X^i	Dissociation constant for binding of solute X to its site on transporter i defined explicitly in Eqs. 3–8 (mM)
ψ_1	Apical membrane potential (cell–lumen)(mV)
ψ_2	Basolateral membrane potential (cell–capillary)(mV)
ψ_t	Transepithelial potential ($\psi_1 - \psi_2$)(mV)
U_i	Dimensionless membrane potentials ($U_i = \psi_i F/RT$)

MODEL FORMULATION

Overview

As shown in Fig. 1, the proximal tubule consists of a single layer of cells with transcellular and paracellular permeation pathways. For each transport pathway shown, the electrokinetic equation describing transporter turnover (picomoles per millimeter tubule length per minute) as a function of solute activities and membrane potential will be used to calculate solute fluxes. Affinities for solute saturability and allosteric dependences will be obtained from reported experimental data; where data are not available, transporters will be assumed to be nonsaturable and not regulated allosterically. The permeability coefficient for each transporter will be determined from measured transcellular flux data and from requirements of intracellular solute balance in steady-state control conditions. Because studies in the proximal tubule are not performed under voltage-clamp conditions, the model must satisfy open circuit boundary conditions, which require equal apical and basolateral currents and equal opposing transcellular and paracellular currents. An iterative procedure will be used to calculate apical and basolateral membrane potentials from solute fluxes. The time course of cell solute concentration, pH, and volume will be calculated by numerical integration of the transport equations.

The major purpose of the model was to examine interactions among H^+/HCO_3, Na, and cell membrane poten-

tials. Because there was relatively little definitive data on cell membrane Cl transporters and on mechanisms of cell volume regulation, Cl and cell volume were kept constant for the simulations shown. In addition, values for the osmotic and reflection coefficients for cell solutes are unknown. For some calculations, however, cell volume was allowed to vary using estimated values for cell solute osmotic coefficients and assumed unity reflection coefficients. Therefore the mathematics of the model was developed to include osmotic water movement. Calculated time courses of cell membrane potentials, pH, and Na were unchanged qualitatively when volume was allowed to vary; quantitative effects of allowing cell volume to vary are given in the Results section. The constant cell Cl and volume assumption is acceptable because (*a*) Cl transport mechanisms are electroneutral on both membranes; (*b*) the major H^+/HCO_3 transporters are not coupled to Cl; and (*c*) all perturbations examined were isosmotic.

The calculation of electrodiffusive solute fluxes requires a specific choice for the mathematical form of the electrokinetic flux equations. For nonsaturable single ion conductances that are not regulated allosterically (transporters 2, 3, 12, 13, and 20–24), the ion flux is given by (Lakshminarayanaiah, 1984),

$$J_i = P_i z U([X]_a - [X]_b e^{-zU}) / (1 - e^{-zU}). \quad (1)$$

J_i is the flux of solute X (with charge z) from side a to side b of a membrane where the concentrations of X are $[X]_a$ and $[X]_b$, P_i is a permeability coefficient, and U is a dimensionless membrane potential defined above.

For coupled electrodiffusive transport processes having substrate saturability and allosteric regulation, there is no rigorous formulation for the form of the transport equations. We have chosen a mathematical form of these equations that contains electrochemical driving forces as predicted from nonequilibrium thermodynamics, and allosteric and saturability terms as normally used in kinetic formulations. For coupled cotransport of n molecules of X^{+z} and m molecules of Y^{+w}, the flux (number of transporter turnovers) is,

$$J_i = \frac{P_i([X]_a, [Y]_a, \ldots)(nz+nw)U([X]_a^n[Y]_a^m - [X]_b^n[Y]_b^m \exp(nz+mw)U)}{(1-\exp(nz+mw)U)\{(1+[X]_a/K_1+\ldots)^n \ldots (1+[Y]_a/K_2+\ldots)^m\}} \quad (2)$$

The permeability coefficient, $P_i([X]_a, [Y]_a, \ldots)$, is regulated allosterically by one or more variables by specifying a functional form for P_i. The electrochemical driving force is expressed as the difference of the products of the concentrations of ligands participating in the transport process weighted by the electrical term, $\exp(nz + mw)U$. The particular form of the generalized saturability term (braced term in the denominator) is selected from known transport mechanisms (Segel, 1975). For multi-ion transport involving independent sites for each substrate molecule, the saturability term consists of a product of terms of the form $(1 + [X]_a/K_1)$; for transport involving a common ion site for many substrates (for example, the Na/H countertransporter) the saturability term takes the form of a summation $(1 + [X]_a/K_1 + [Y]_a/K_2 + [X]_b/K_3 + \ldots)$. In the absence of allosteric regulation, saturability, and coupled transport, Eq. 2 reduces to Eq. 1. Eq. 2 predicts $J_i = 0$ when $[X]_a^n[Y]_a^m = [X]_b^n[Y]_b^m \exp((nz + mw)U)$ as expected. Because of the terms in the denominator, Eq. 2 also gives saturation in J_i with increasing solute concentrations. As discussed below, simplified forms of Eq. 2 are used to describe each transport system with the exception of the ATPases.

Based on the rapid diffusibility of CO_2, it is assumed that pCO_2 is constant throughout the epithelium (Schwartz et al., 1981; Lucci et al., 1982). It is also assumed that the specified compositions of the luminal and peritubular fluid do not change with changes in cell fluid composition. This is valid because of the small cell volume and rapid luminal and peritubular flow used in the experiments simulated. Cell and extracellular unstirred layer effects are neglected.[1]

SELECTION OF MODEL PARAMETERS

Cell Membrane Transporters

Na/H Antiporter. Based on data from Aronson and colleagues (Aronson et al., 1983), luminal H and Na compete for a single binding site. This site was saturable with respect to Na ($K^0_{Na} = 7.1$ mM in the theoretical absence of H) and luminal H ($K^0_H = 3.8 \times 10^{-5}$ mM). It is assumed that the cell Na binding site is also saturable with the same affinity (K^0_{Na}). The measured allosteric dependence of Na/H transport on cell pH was included in the functional form $P_0(pH) = P_0(1 + 2{,}400[H])$ based on the data of Aronson et al. (1982),

$$J_0 = \frac{P_0(1 + 2{,}400[H])\,([Na]_l[H] - [Na][H]_l)}{1 + [H]_l/K^0_H + ([Na] + [Na]_l)/K^0_{Na}}. \quad (3)$$

P_0 (see Table I) was chosen to give H efflux rates equal to ~85% of the rate of transepithelial proton secretion measured under control conditions (Alpern, 1984). This was chosen on the basis of data by Bank et al. (1985) where DCCD (dicyclohexylcarbodiimide, an inhibitor of H-

[1]As noted above, Eq. 1 was used to describe paracellular ion movement. This equation does not include a solvent drag term. Although Fromter et al. (1973) and Bomsztyk and Wright (1986) have demonstrated solute–solvent interactions in the proximal tubule, we found that for HCO_3 movement, these interactions required the presence of active transport (Alpern, 1984), and thus could not represent solvent drag across the tight junction. Our data were most compatible with a solute–solvent interaction in the renal interstitium, which secondarily affected transcellular transport, and, in the case of more permeant ions, paracellular diffusive rates. In the present model we have not included extracellular unstirred layers since these are poorly defined and would add much complexity to the model.

TABLE I
TRANSPORTER PERMEABILITIES AND STEADY-STATE FLUXES

Transporter	P_i	Units	Steady-state flux
			pmol/mm·min
Apical membrane			
0. Na/H	395,000	nl^2/pmol·mm·min	131.8
1. Na/glucose	0.044	nl^2/pmol·mm·min	132.8
2. H	55,200	nl/mm·min	6.7
3. K	7	nl/mm·min	−41.8
4. H-ATPase	0.0037	pmol/mm·min·mV	22.4
5. H_2O		nl^2/pmol·mm·min	
Basolateral membrane			
10. $Na/3HCO_3$	0.0815	nl^4/$pmol^3$·mm·min	46.8
11. Glucose	14	nl/mm·min	132.8
12. K	18.4	nl/mm·min	94.4
13. H	55,200	nl/mm·min	−7.0
14. 3Na/2K ATPase	10,015	pmol/mm·min	72.6
15. K/Cl	0.012	nl^2/pmol·mm·min	8.9
16. H_2O		nl^2/pmol·mm·min	
Paracellular pathway			
20. Na	10.6	nl/mm·min	−72.7
21. K	11.7	nl/mm·min	−2.7
22. Cl	8.6	nl/mm·min	51.8
23. HCO_3	1.6	nl/mm·min	2.6
24. Choline	1.7	nl/mm·min	

ATPase) was found to inhibit 15% of transepithelial proton secretion.

Proton Translocating ATPase. The existence of an apical membrane proton translocating ATPase has been suggested by a number of investigators (Bank et al., 1985; Chan and Giebisch, 1981; Howlin et al., 1985; Kinne-Saffran et al., 1982; Schwartz and Al-Awqati, 1985). Although it is not settled what fraction of apical membrane proton efflux is mediated by a H-ATPase, we chose 15% in the control condition based on the data of Bank et al. (1985). To model the kinetics of the H-ATPase, we assumed that its rate is determined by the electrochemical driving forces, offset by a constant energy provided by the pump.

$$J_2 = P_2(zF_1/RT + \Delta pH + zF\psi_{pump}/RT). \quad (4)$$

ψ_{pump} is the electrochemical energy provided by the pump, which was taken to be 120 mV (2 pH units).

H Conductive Pathways. The apical and basolateral membranes contain small H conductances of similar magnitudes as shown in membrane vesicle studies (Verkman and Ives, 1986*a*; Verkman, 1987). Based on studies in the in vivo microperfused tubule, the basolateral membrane H conductances comprise less than 10% of Na-coupled H fluxes under control conditions (Alpern, 1985). Eq. 1 was used to describe the diffusive H fluxes and has been found to be valid for small pH gradients ($\Delta pH < 1$ unit) and electrical potentials (<80 mV) in isolated brush border membrane vesicles (Verkman and Ives, 1986*a*).

K Pathways. The apical K conductance was described by Eq. 1 with P_3 chosen to give a flux equivalent to that predicted by a conductance of 0.0039 mho/cm^2 measured by Fromter (1982) for the apical membrane in the absence of luminal organic solutes. Fromter (1984) found that the predominant apical membrane conductance is a K conductance in the absence of luminal organics.[2]

Basolateral K conductance was also described by Eq. 1 with P_{12} chosen to give a K flux under control conditions equal to that predicted by a K conductance of 0.0075 mho/cm^2, which is ~70% of the basolateral membrane conductance measured by Fromter (1982). The K conductance was also regulated allosterically by peritubular pH based on studies in the rabbit proximal tubule by Biagi and Sohtell (1986). Interestingly, regulation of K conductance by peritubular pH was necessary to prevent marked cell K depletion when peritubular pH was lowered. Based on the data of Biagi and Sohtell, the flux equation is

$$J_{12} = P_{12}(0.82pH_2 - 5.06)U_2 \cdot ([K]_2 - [K]e^{-U_2})/(1 - e^{-U_2}). \quad (5)$$

Although Cl transporters were not used in the basic model, a small basolateral neutral K flux (see Table I) was required for the model to achieve a stable steady state. The neutral K flux was coupled to fixed Cl according to the equation,

$$J_{15} = P_{15}([K][Cl] - [K]_2[Cl]_2). \quad (6)$$

J_{15} did not contribute to basolateral membrane current and hence has no effect on membrane potential.

Organic Solute Transport. On the apical membrane, the glucose and amino acid transporters are coupled

[2]In this model we have attributed all of the apical membrane conductance observed in the absence of luminal organic solutes to a K conductance, as suggested by Fromter (1984). Kawahara (1985) also found a large apical membrane K conductance in the newt proximal tubule. While Lapointe et al. (1986) have not found a large apical membrane K conductance in the rabbit proximal tubule, these authors could not account for 60% of their measured apical membrane conductance. Because of the large apical membrane K conductance, the model predicts a significant amount of net K secretion (42 pmol/mm · min). While microperfusion studies have found K secretion in the rabbit proximal straight tubules perfused with ultrafiltrate-like solutions (Wasserstein and Agus, 1983), the rates were much smaller than those predicted by the model. In addition, micropuncture studies along the entire proximal tubule usually find net K absorption. While the exact mechanism of apical membrane conductance remains unclear, at present K seems to be the best choice.

1:1 to Na. We lumped all electrogenic Na-coupled transporters together as a nonsaturable "Na/glucose" transporter (Hopfer and Groseclose, 1980). P_1 was chosen to give a net rate for Na-coupled organic transport of 140 pmol/mm · min.

$$J_1 = \frac{P_1 U_1([\mathrm{Na}]_1[\mathrm{glucose}]_1 - [\mathrm{Na}][\mathrm{glucose}]e^{-U_1})}{(1 - e^{-U_1})}. \quad (7)$$

The exit pathways for glucose and amino acids were taken to be neutral (Fromter, 1979) and nonsaturable with J_{11} chosen to give equal apical and basolateral membrane glucose/amino acid fluxes in steady-state control conditions.

$Na/3HCO_3$ Cotransporter. This was the major basolateral membrane HCO_3 exit step with a 1:3 Na to HCO_3 coupling ratio (Alpern, 1985; Yoshitomi et al., 1985). Its rate was a saturable function of peritubular Na ($K^{10}_{Na} = 10$ meq/liter) and peritubular HCO_3 ($K^{10}_{HCO_3} = 10$) as shown by Akiba et al. (1986).

$$J_{10} = \frac{2P_{10}U_2([\mathrm{Na}]\,[\mathrm{HCO_3}]^3 e^{-2U_2} - [\mathrm{Na}]_2[\mathrm{HCO_3}]_2^3)}{(1 - e^{-2U_2})(1 + [\mathrm{Na}]_2/K^{10}_{Na})(1 + [\mathrm{HCO_3}]_2/K^{10}_{HCO_3})^3}. \quad (8)$$

P_{10} was chosen to match apical and basolateral H fluxes in the steady state under control conditions.

3Na/2K-ATPase. This was included in the model as a voltage-independent transporter in a manner similar to that of Latta et al. (1984):

$$J_{14} = P_{14}([\mathrm{Na}]/([\mathrm{Na}] + K^{14}_{Na}))^3([\mathrm{K}]_2/([\mathrm{K}]_2 + K^{14}_{K}))^2. \quad (9)$$

The rate was a saturable function of intracellular Na ($K^{14}_{Na} = 50$ mM; Jorgensen, 1980) and peritubular K ($K^{14}_{K} = 1.1$ mM; Jorgensen, 1980). P_{14} was chosen to match steady-state apical and basolateral membrane Na fluxes under control conditions.

Osmotic Water Transport. Based on tubule microperfusion and membrane vesicle measurements, both the apical and basolateral membranes have high osmotic water permeabilities ($P_f \sim 0.1$ cm/s; Verkman et al., 1985; Verkman and Ives, 1986*b*; Meyer and Verkman, 1987). Volume flux (J_6, J_{17}) is described by the equations,

$$J_5 = P_6(\Phi_{[1]} - \Sigma(\phi_X/a_X)[X]) \quad (10a)$$

$$J_{16} = P_{17}(\Phi_{[2]} - \Sigma(\phi_X/a_X)[X]), \quad (10b)$$

where $\Phi_{[1]}$ and $\Phi_{[2]}$ are osmolarities of the luminal and peritubular fluids, respectively, and ϕ_X is the intracellular osmotic coefficient of solute X assumed to be 0.7 for charged solutes and 1 for glucose. P_6 and P_{17} were determined from the product of P_f (0.1 cm/s), the partial molar volume of water (18 cm^3/mol), and average tubule surface area (1.1×10^{-3} cm^2/mm).

Paracellular Pathway

Paracellular fluxes were taken as nonsaturable functions of luminal and peritubular solute concentrations according to Eq. 1. Permeability coefficients P_{20} to P_{24} were obtained from reported measurements (Fromter, 1977; Alpern et al., 1982).

Fluid Compositions

The compositions of luminal, cell, and capillary fluids under steady-state control conditions are given in Table II. Both concentrations and activities are given. Cell Na, K, and Cl concentrations and activity coefficients were determined from reported microelectrode (Yoshitomi and Fromter, 1985; Yoshitomi et al., 1985; Edelman et al., 1978; Cassola et al., 1983) and microprobe measurements (Thurau et al., 1979; Beck et al., 1980). Cell pH was determined from fluorescence dye (Alpern, 1985) and microelectrode studies (Yoshitomi and Fromter, 1984). The compositions of the luminal and capillary fluids were chosen to resemble those used to simulate the early rat proximal tubule in microperfusion studies (Alpern et al., 1982). As discussed above, "glucose" refers to all Na-coupled neutral species including glucose and the amino acids. Extracellular impermeants have been included to simulate the experimental conditions of Na replacement by choline. Intracellular impermeants are required to give zero volume flow across cell membranes under steady-state control conditions.

NUMERICAL SOLUTION

The computational procedure used to determine the time course of cell solute concentrations, pH, and volume is diagrammed schematically in Fig. 2. Initial solute concentrations and changes in fluid compositions for simulated experiments are specified by the fluid composition controller. The neutral fluxes that do not depend upon ψ_1 and ψ_2

TABLE II
COMPOSITIONS OF CELL AND TUBULE FLUIDS

	Lumen	Cell	Capillary
Na	107 (147)	13 (22)	107 (147)
K	3.65 (5)	82 (136)	3.65 (5)
Cl	94 (129)	13 (33)	94 (129)
Glucose	10	20	10
pH	7.32	7.13	7.32
pCO_2	50	50	50
Impermeant	0	126	0
Osmolarity	291	291	291

Solute activities are in millimolars. Values in parentheses are total solute concentrations; the activity coefficient is the ratio of solute activity to total solute concentration. For calculations in which cell volume was allowed to vary, an intracellular impermeant was added to give zero volume flow under steady-state control conditions. For charged solutes, osmotic coefficients were assumed to be 0.92 in the lumen and capillary, and 0.7 in the cell.

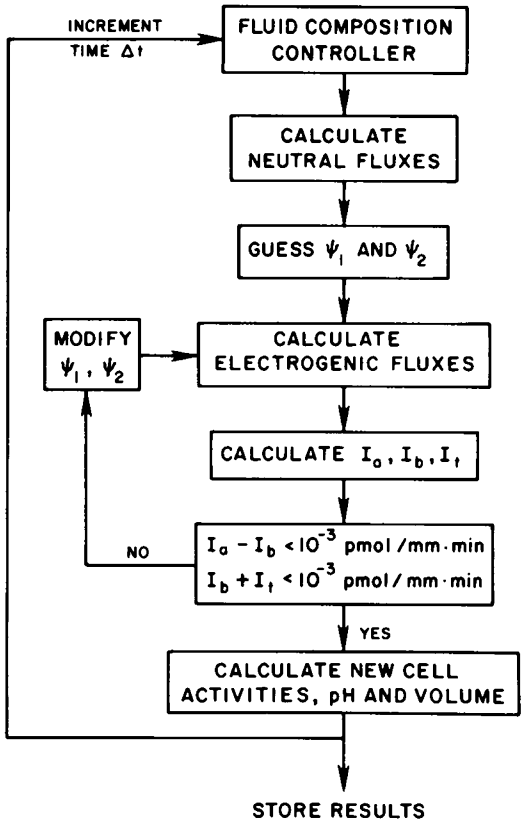

FIGURE 2 Method for numerical solution.

(transporters 0, 5, 11, 15, and 16) are calculated using a first order forward Newton's method. Based on initial guesses for ψ_1 and ψ_2, the remaining electrogenic fluxes are calculated. For a dimensionless potential U_1 or $U_2 < 0.1$, a Bernoulli expansion was required for acceptable numerical precision (Dwight, 1961),

$$U/(1 - e^{-U}) = 1 + U/2 + U^2/12 + U^4/720. \quad (11)$$

Transmembrane net currents (I_1 and I_2) and the paracellular current (I_t) are calculated from transporter fluxes,

$$I_1 = J_1 + J_2 + J_3 - J_4 \quad (12a)$$

$$I_2 = -2J_{10} + J_{12} + J_{13} + J_{14} \quad (12b)$$

$$I_t = J_{20} + J_{21} - J_{22} - J_{23} + J_{24}, \quad (12c)$$

where positive current is defined as positive charge movement in the lumen to capillary direction. U_1 and U_2 are determined iteratively from the requirements of cell electroneutrality ($I_1 = I_2$) and equal opposing transcellular and paracellular currents ($I_2 = -I_3$) using the generalized Newton method (Young and Gregory, 1973). This approach was found to give rapid convergence with $<10^{-3}$ pmol/mm · min current differences ($I_1 - I_2$ and $I_2 + I_3$) in two to three iterations for initial membrane potential guesses between 0 and -100 mV. Fitted U_1 and U_2 values at time t were used as the initial guesses for the calculation at time $t + \Delta t$.

Transporter fluxes determined from the fitted membrane potentials are used to calculate changes in cell volume and solute concentrations,

$$V(t + \Delta t) = V(t) + (J_5 - J_{16})\,\Delta t \quad (13a)$$

$$\mathrm{Na}(t + \Delta t) = [\mathrm{Na}(t)V(t) + a_{\mathrm{Na}}(J_0 + J_1 - J_{10} - 3J_{14})\Delta t]/V(t + \Delta t) \quad (13b)$$

$$\mathrm{K}(t + \Delta t) = [\mathrm{K}(t)V(t) + a_{\mathrm{K}}(J_3 - J_{12} + 2J_{14} - J_{15})\Delta t]/V(t + \Delta t) \quad (13c)$$

$$\mathrm{glucose}(t + \Delta t) = [\mathrm{glucose}(t)V(t) + (J_1 - J_{11})\Delta t]/V(t + \Delta t), \quad (13d)$$

where Δt is the integration interval and a_X is the activity coefficient for solute X in the cell. The new cell pH is calculated from net movement of H equivalents into the cell and the cell buffer capacity (B(pH)),

$$\mathrm{pH}(t + \Delta t) = \mathrm{pH}(t) + (-J_0 + J_2 - J_4 + 3J_{10} - J_{13})\Delta t/B\,(\mathrm{pH}) - [\mathrm{HCO_3}(t)][1 - V(t)/V(t + \Delta t)]V_0)/B(\mathrm{pH}). \quad (13e)$$

B(pH) was taken to be 8.84×10^{-8} mmol/mm · pH unit based on the measured proximal tubule cell buffer capacity of 65 mmol/liter · pH unit measured by Yoshitomi et al. (1985) and the conversion $V_0 = 1.36$ nl cell volume/mm tubule length. An alternate form for tubule cell buffer capacity would be to sum the separate contributions from HCO_3 buffer capacity ($2.3[HCO_3]$) and non-HCO_3 buffer capacity; we chose to use the constant B(pH) for all calculations. The $[HCO_3][1 - V(t)/V(t + \Delta t)]$ term is required because changes in cell $[HCO_3]$ occur with changes in cell volume. The cell $[HCO_3]$ at time $t + \Delta t$ is calculated from cell pH($t + \Delta t$) and the assumed constant pCO_2 conditions, $[HCO_3] = 2.4 \times 10^{(\mathrm{pH}-5)}pCO_2$, with pCO_2 expressed in mm Hg and $[HCO_3]$ in mM. The new cell parameters at time $t + \Delta t$ are then used to continue the integration.

The model was implemented on a PDP MINC/23 computer (Digital Equipment Corp., Maynard, MA) using the MINC-11 basic operating system in single precision. The computation time per increment in time was generally ~0.3 s; 100–300 time intervals were chosen for most integrations. Decreasing Δt 10-fold had no effect on the calculated time courses.

The steady-state fluxes for each transporter are given in Table I for the basic model in which transcellular Cl and all water movement were absent. Membrane potentials, solute concentrations, and pH remained constant (<0.01% change) for a 5-min integration time.

RESULTS

The model was developed initially to examine the complex interrelations involved in cell pH regulation in the mammalian proximal tubule, an epithelium with large transcellular proton fluxes. Because cell pH is affected by a wide

variety of transporters whose rate is modulated by intra- and extracellular pH, Na concentration, and electrical potential, it became necessary to develop a more complete model of the proximal tubular cell. While the model presented here does not include all proximal tubular transport processes, it includes all of those that have major effects on cell pH, [Na], and cell potentials. In this section we first demonstrate that the predictions of the model were in agreement with some basic findings in the intact mammalian proximal tubule. Since parameters were chosen primarily from results in the rat proximal tubule, model predictions were compared with results in this species when available.

Regulation of Apical (ψ_a) and Basolateral (ψ_{bl}) Membrane Potential

The electrical characteristics of the model were compared with those of the intact tubule. Under steady-state control conditions (with ultrafiltrate-like solutions in luminal and peritubular compartments), ψ_{bl} was -70.00 mV, ψ_a -69.03 mV, and ψ_t -0.97 mV. These results agree well with the results of Fromter and colleagues in the rat proximal convoluted tubule (Fromter, 1984). The ratio of apical to basolateral resistances (R_a/R_{bl}) was 2.1 as determined from the voltage divider ratio calculated under 0 and 5 mV voltage clamp conditions. The major fractional change in current, induced as transepithelial voltage was increased from 0 to 5 mV, occurred on the apical K (0.66) and basolateral K (0.81) conductances with other major contributions from apical Na/glucose (0.27) and basolateral Na/3HCO_3 cotransport (0.16).[3]

Regulation of Cell pH

Because cell pH is regulated by at least five transporters (apical Na/H antiporter, H-ATPase, and H leak and basolateral Na/3HCO_3 cotransporter and H leak), regulation of cell pH is extremely complex and requires mathematical modelling.

Fig. 3 shows the effect on cell pH of changing peritubular or luminal HCO_3 concentration by 20 meq/liter at constant CO_2 tension. Changes in peritubular pH affect cell pH to a greater extent than similar changes in luminal pH. This is similar to results observed previously. When

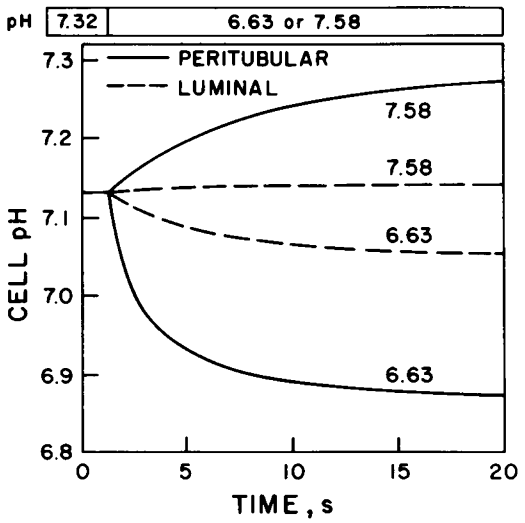

FIGURE 3 Response of cell pH to perturbations in extracellular pH. Cell pH was calculated as a function of time. Luminal (*dashed line*) or peritubular (*solid line*) pH was changed at the indicated time. Calculations in this and subsequent figures performed with fixed cell volume. When volume was allowed to vary, cell pH at 20 s changed by <0.01 units. The maximum change in cell volume was -7% when peritubular pH was decreased to 6.63.

peritubular HCO_3 concentration was decreased by 20 meq/liter, cell pH decreased by 0.25–0.35 pH units, while a similar decrease in luminal HCO_3 concentration caused cell pH to decrease by 0.08–0.10 pH units (Alpern, 1985; Alpern and Chambers, 1986). In addition, in studies in the in vivo microperfused tubule, cell pH changed with a $t_{1/2}$ of less than 5 s (Alpern, 1985; Yoshitomi and Fromter, 1984), in agreement with the rapid time course predicted by the model.

Fig. 3 also shows that decreases in extracellular HCO_3 concentration have a greater effect on cell pH than do increases, similar to findings in the in vivo tubule. When peritubular HCO_3 concentration was decreased from 25 to 5 meq/liter, cell pH decreased by 0.25–0.35 pH units (Alpern, 1985; Alpern and Chambers, 1986), whereas increased peritubular HCO_3 (25–45 meq/liter) caused cell pH to increase by 0.10 pH units (mean ± SE: 7.14 ± 0.02 vs. 7.24 ± 0.02; $n = 6$; $P < 0.001$; unpublished observation). The greater sensitivity of the apical membrane Na/H antiporter and H-ATPase to decreasing HCO_3 concentration occurs because decreases in luminal HCO_3 concentration are associated with larger changes in proton concentration, the major rate determinant. The greater sensitivity of the basolateral membrane Na/3HCO_3 transporter occurs because of its saturability in HCO_3 (K_m = 10 meq/liter), as reported in basolateral membrane vesicle studies (Akiba et al., 1986).

Fig. 4 shows the effect of luminal or peritubular acidification on ψ_a and ψ_{bl}. Luminal acidification affects minimally ψ_a and ψ_{bl} in agreement with the results of Burckhardt et al. (1985*b*). Peritubular acidification caused a spike depolarization to -28 mV, which relaxed with a $t_{1/2}$

[3]Transference numbers for each of the transporters were calculated from the fractional change in current across each transporter when clamped transepithelial voltage was increased from 0 to 5 mV. Interestingly, these transference numbers were slightly different from those calculated from changes in ψ_{bl} in response to concentration jumps. To examine the mechanism of this discrepancy, we created a simplified model with a few simple transporters across a single barrier. In this setting, transference numbers were identical by both methods, whether the transporters were simple, coupled, or saturable. A discrepancy developed when a baseline current existed. Strickholm and Wallin (1967) have previously discussed the fact that the calculation of transference numbers from concentration jump is based on zero net membrane current, a condition not present in the model or in the proximal tubule.

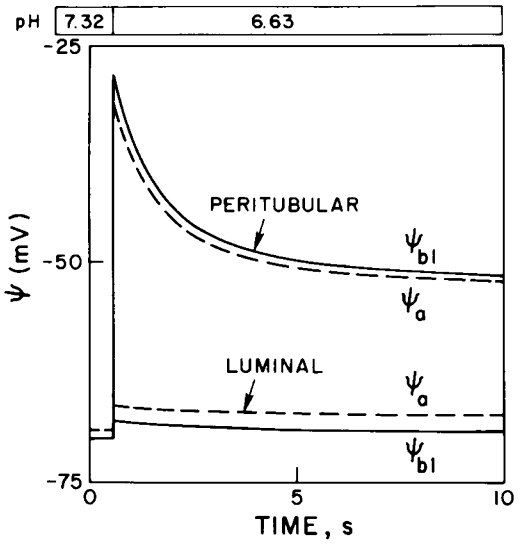

FIGURE 4 Time course of cell membrane potentials after a decrease in extracellular pH. Apical (*dashed line*) and basolateral (*solid line*) membrane potentials were calculated after a decrease in peritubular (*upper traces*) or luminal (*lower traces*) pH.

of ~2 s to −50 mV. This large depolarization with the late relaxation agrees with electrophysiological results in the intact tubule (Burckhardt et al., 1984*b*). Yoshitomi and Fromter (1984) found that the relaxation of the membrane potential after the spike occurred with a $t_{1/2}$ of 2.1 s. Comparing Figs. 3 and 4, it is seen that the time course of the ψ_{bl} relaxation is similar to the time course of cell acidification, which is the major cause of the repolarization.

In microperfusion studies, changes in extracellular Na concentration have complex effects on cell pH. When peritubular Na concentration is lowered, cell pH decreases by approximately 0.2 pH units with a $t_{1/2}$ of less than 5 s (Yoshitomi et al., 1985; unpublished observation). The model also predicts a monotonic decrease in cell pH with a rapid time course ($t_{1/2}$ ~2 s). In microperfusion experiments, lowering peritubular Na concentration is also associated with a spike depolarization that relaxes with $t_{1/2}$ similar to that observed for cell acidification (Yoshitomi et al., 1985). The model also predicted this behavior (Fig. 5). These effects on cell pH and cell potential are due primarily to the electrogenic $Na/3HCO_3$ cotransporter.

Luminal Na removal has more complex effects on cell pH. In microperfusion studies, luminal Na removal had a biphasic effect on cell pH, initially acidifying the cell and then alkalinizing the cell in the steady state (Alpern and Chambers, 1986). The initial acidification was thought to result from reversal of the Na/H antiporter and increased basolateral membrane $Na/3HCO_3$ cotransport secondary to cell hyperpolarization. The cell hyperpolarization in response to luminal Na removal (Fig. 5) is due to slowing and/or reversal of the Na-coupled organic solute cotransporter. Removal of organic solutes from the luminal perfusate decreased the magnitude of, but did not eliminate, the initial acidification and the late alkalinization (Alpern and Chambers, 1986).

The late alkalinization is more complex. Inhibition of the basolateral membrane $Na/3HCO_3$ cotransporter with peritubular 4-acetamido-4′-isothiocyanostilbene-2,2′-disulfonate inhibited the late alkalinization (Alpern and Chambers, 1986). However, based on thermodynamic considerations, it was not clear whether the $Na/3HCO_3$ cotransporter could actually reverse and supply alkali to the cell. To examine this problem, the effect of luminal Na removal on cell pH in the absence of luminal organic solute was studied. The model predicted a biphasic time course with initial acidification and late alkalinization (Fig. 6, line labeled 0.15). However, the magnitude of the late alkalinization was smaller than that observed in microperfusion experiments in that cell pH never increased above the control level (Alpern and Chambers, 1986).

When selecting model parameters, the fraction of apical membrane proton secretion mediated by a H-ATPase was not known (see Model Formulation). As the H-ATPase was a likely source for the alkali during the cell alkalinization, we examined the effect of varying the magnitude of the H-ATPase on the response to luminal Na removal (Fig. 6). When apical membrane proton secretion was mediated completely by Na/H exchange with no H-ATPase, the biphasic response and late alkalinization were eliminated. Increasing the proportion of proton secretion mediated by H-ATPase increased the magnitude of the late alkalinization. The data were best fit by ~30% H-ATPase. To examine further the components of the biphasic response to luminal Na removal, we modified the model such that 30% of apical membrane proton secretion was mediated by H-ATPase.

Fig. 7 shows the effect of SITS (setting the rate of the $Na/3HCO_3$ to zero) on the biphasic response of cell pH to

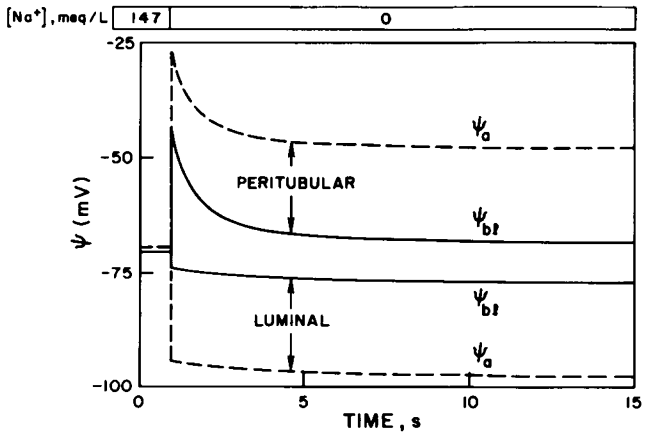

FIGURE 5 Response of cell membrane potentials to extracellular Na removal. Apical (*dashed line*) and basolateral (*solid line*) membrane potentials were calculated after removal of peritubular (*upper traces*) or luminal (*lower traces*) Na. When cell volume was allowed to vary, peak and 15 s potentials changed by less than 2 mV. There was less than 8% change in cell volume for each perturbation.

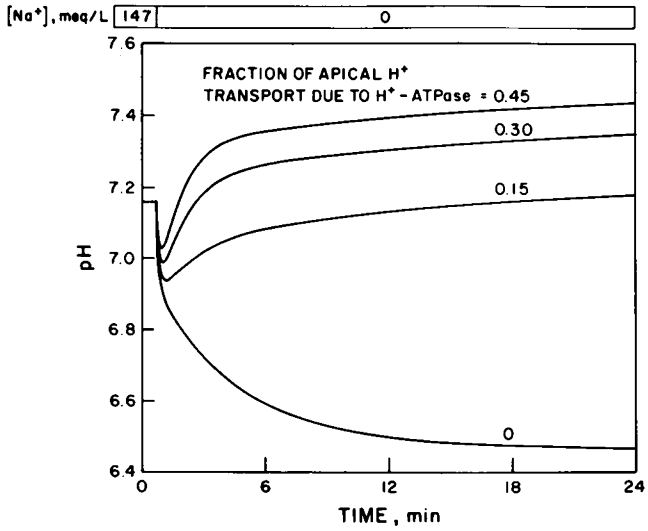

FIGURE 6 Response of cell pH to luminal Na removal: role of apical H-ATPase. Cell pH was calculated as a function of time after removal of luminal Na. Each curve represents model calculations in which the fraction of apical H transport mediated by the H-ATPase is indicated. For each calculation, P_0 was adjusted to maintain constant apical membrane H transport and P_{14} was adjusted to give identical cell Na concentrations before luminal Na removal.

luminal Na removal.[4] In microperfusion experiments performed under control conditions, luminal Na removal caused a 0.04 pH unit acidification followed by a late alkalinization of 0.11 pH units (Alpern and Chambers, 1986). In the presence of peritubular SITS, luminal Na removal caused a 0.25 pH unit decrease in cell pH with no late alkalinization (Alpern and Chambers, 1986). Although the cell pH changes predicted by the model are somewhat larger than those observed, the patterns are very similar.

Fig. 8 shows the individual fluxes contributing to the biphasic cell pH response. Alkalinizing fluxes are shown as positive. Under steady-state control conditions, most of proton efflux is mediated by Na/H exchange with some mediated by the H-ATPase. Most proton influx is mediated by $Na/3HCO_3$ cotransport with a small contribution from H conductances. Luminal Na removal causes an immediate reversal of the Na/H antiporter, which causes the initial cell acidification. This is followed by secondary changes in the rate of the Na/H antiporter and the $Na/3HCO_3$ cotransporter in response to the altered cell pH and Na concentration. The major alkalinizing flux during the late alkalinization is mediated by the H-ATPase. However, if HCO_3 efflux (equivalent to proton entry) on the $Na/3HCO_3$ cotransporter did not slow, the

[4]In the experiments where SITS was added to the peritubular capillary, peritubular bicarbonate concentration was lowered to 5 meq/liter to prevent marked cell alkalinization (Alpern and Chambers, 1986). In this setting, there is a significant rate of proton influx across the basolateral membrane driven by the large pH and electrical gradients. The model was implemented under similar conditions.

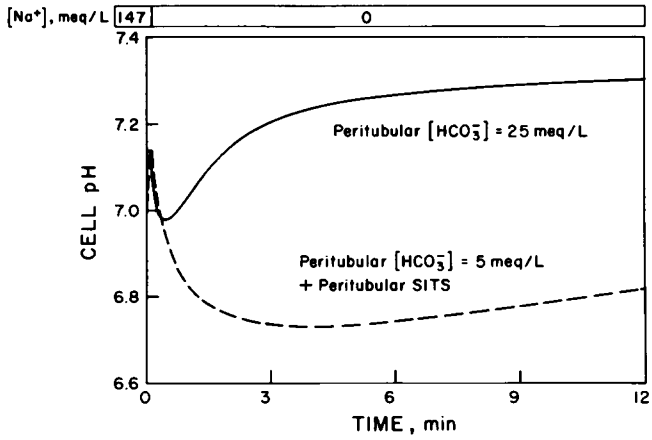

FIGURE 7 Response of cell pH to luminal Na removal: role of basolateral $Na/3HCO_3$ cotransport. Cell pH was calculated as a function of time after luminal Na removal. Solid curve is identical to that labeled 0.30 in Fig 6. Dashed curve was calculated with J_{10} ($Na/3HCO_3$) set to zero (SITS inhibition). Peritubular HCO_3 was 5 meq/liter.

flux from the H-ATPase would not be sufficiently large to alkalinize the cell. Thus the late alkalinization is due to a relatively constant H-ATPase and a large change in the rate of the $Na/3HCO_3$ cotransporter. These results thus provide evidence for: (*a*) a significant contribution of apical membrane H-ATPase to apical membrane proton efflux; and (*b*) regulation of the rate of basolateral membrane $Na/3HCO_3$ cotransporter by cell composition. In in vivo microperfusion studies designed to examine the effect of luminal amiloride and more potent amiloride analogues on the rates of HCO_3 absorption, Preisig et al. (1986) concluded that ~65% of apical membrane proton secretion is mediated by the Na/H antiporter, while the remaining 35% is mediated by a different process, most likely an H-ATPase. These conclusions are similar to those of the present model (~30% H-ATPase).

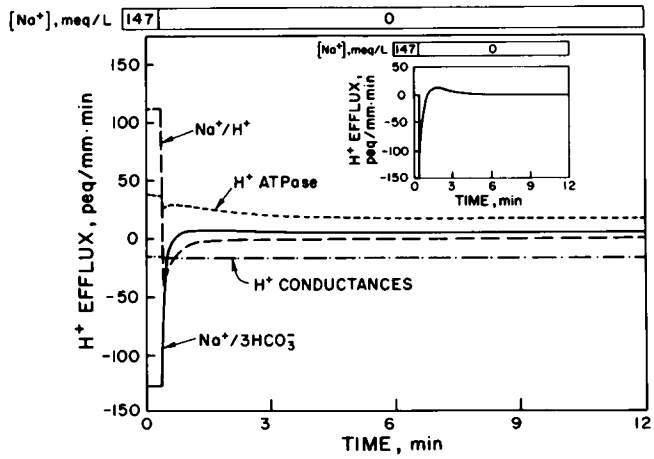

FIGURE 8 Time course of H fluxes after luminal Na removal. H fluxes were calculated as a function of time after luminal Na removal. Positive fluxes represent cell H efflux (or equivalently HCO_3 influx). A composite curve labeled "H conductances" contains the sum of apical and basolateral H conductances. Insert shows the total H efflux.

In a number of epithelial systems (salamander and mammalian proximal tubules, bovine corneal endothelium), there appears to be an association of an Na/H antiporter on one membrane with an electrogenic Na/$3HCO_3$ cotransporter on the opposite membrane (Alpern, 1985; Alpern and Chambers, 1986; Boron and Boulpaep, 1983; Biagi, 1985; Jentsch et al., 1984; Sasaki et al., 1986). A possible reason for the association of these two transporters is protection of cell pH. Under physiological conditions, luminal pH can vary up to 0.7 pH units along the length of the proximal tubule. In the steady state, this is associated with changes in the rate of the apical and basolateral membrane transport mechanisms (Alpern, 1984; Alpern et al., 1982). A slowing or acceleration of the Na/H antiporter, which alters cell pH, will cause a change in rate of the $Na/3HCO_3$ transporter. If the $Na/3HCO_3$ transporter could respond to changes in cell Na concentration secondary to changes in Na/H antiporter rate, then smaller changes in cell pH would be required.

To test this hypothesis, we compared the effect of luminal pH on cell pH under control conditions, and when the rate of the $Na/3HCO_3$ cotransporter was insensitive to cell Na concentration. As shown in Fig. 9 (*top*), the changes in cell pH were only slightly greater when the $Na/3HCO_3$ cotransporter was insensitive to cell Na concentration. This small effect is due to the small changes in cell Na concentration that occur in response to luminal acidification (~1 meq/liter; Fig. 10 *A*). Thus unless the model is incomplete with regard to regulation of cell Na concentration, this mechanism does not appear to be important.

Another possible reason for Na coupling of the basolateral membrane transporter is to make cell pH independent of luminal organic solute concentration. Under physiological conditions, the early proximal tubule contains many organic solutes that are cotransported with Na electrogenically across the apical membrane. These solutes, high in concentration in the luminal fluid of the early proximal tubule, are absorbed and virtually absent from the late proximal tubule.

Removal of luminal organic solutes will lead to cell hyperpolarization, which secondarily accelerates HCO_3

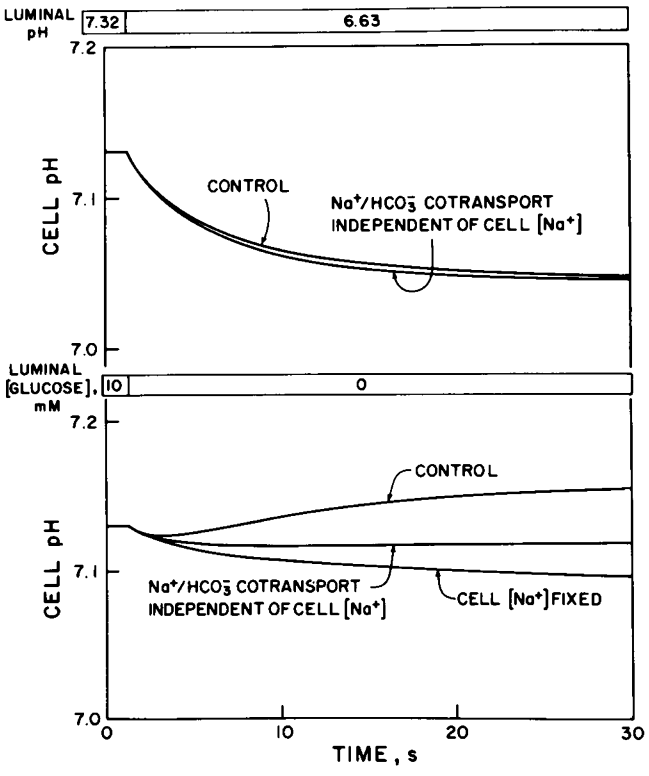

FIGURE 9 Role of Na-coupled transporters in defense of cell pH. (*Top*) Cell pH was calculated as a function of time after luminal acidification. Upper curve is identical to dashed line labeled 6.63 in Fig 3. Lower curve was calculated with [Na] in Eq. 7 fixed to its value in the control condition (13 meq/liter). (*Bottom*) Cell pH was calculated as a function of time after removal of luminal glucose (*upper curve*). In the middle curve [Na] in Eq. 7 was fixed to 13 meq/liter. In the lower curve cell [Na] for all transport (Eqs. 3, 6, 7, and 8) was fixed to 13 meq/liter.

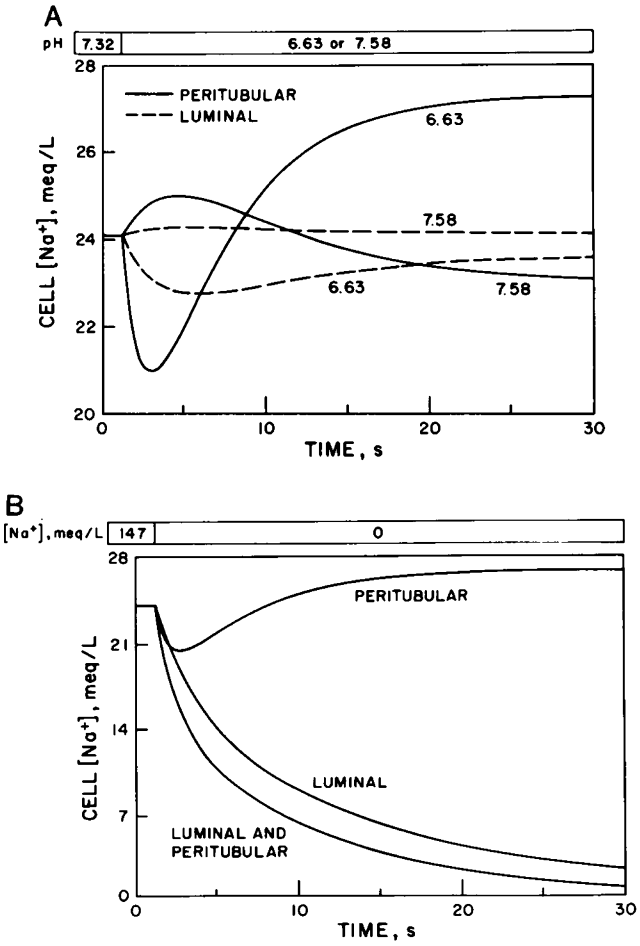

FIGURE 10 Response of cell Na concentration to perturbations in extracellular pH and Na. (*A*) Cell Na concentration was calculated as a function of time. Luminal (*dashed line*) or peritubular (*solid line*) pH was changed at the indicated time. (*B*) Cell Na was calculated as a function of time after removal of Na from the luminal, peritubular, or luminal and peritubular compartments.

efflux across the $Na/3HCO_3$ transporter and leads to cell acidification. However, removal of luminal organic solutes also lowers cell Na concentration, which accelerates proton efflux on the apical membrane Na/H antiporter, and slows HCO_3 efflux on the basolateral membrane $Na/3HCO_3$ cotransporter. Thus, the Na-dependent and potential-dependent effects could cancel partially to make cell pH nearly independent of luminal organic solute concentration.

Fig. 9 (*bottom*) shows that this hypothesis is sound theoretically. The effect of luminal organic solute removal on cell pH was examined first under control conditions, where cell pH was found to transiently acidify and then slightly alkalinize in the steady state. If cell Na concentration was not allowed to change during luminal organic solute removal, there was a significant cell acidification, implying that secondary effects of cell Na concentration on the Na/H antiporter and the $Na/3HCO_3$ cotransporter were key in preventing cell acidification. The individual role of the $Na/3HCO_3$ cotransporter was examined by allowing cell Na concentration to change, but not allowing cell Na concentration to affect the rate of the $Na/3HCO_3$ cotransporter. An intermediate effect was observed (Fig. 9, *bottom*). Thus, this may provide a reason for the presence of a Na-coupled HCO_3 transporter on the basolateral membrane. The importance of this protective effect may be much greater than that shown in Fig. 9 (*bottom*). While we have included one cotransporter to account for Na/glucose and Na/amino acid cotransport, we have probably underestimated the role of these transporters by not including Na-coupled transporters of citrate, succinate, lactate, acetate, and others.

Regulation of Cell [Na]

Fig. 10 *A* shows the effects of extracellular pH on cell [Na]. These results were originally somewhat surprising. Changes in peritubular pH cause a biphasic response in cell [Na]. The first phase is due to changes in the rate of the basolateral membrane $Na/3HCO_3$ cotransporter. The second phase is due to changes in Na/H antiporter rate that occur in response to altered cell pH and dominate in the steady state. In the steady state, each HCO_3 exiting across the apical membrane is accompanied by $\frac{1}{3}$ Na. The proton exiting across the apical membrane is accompanied by 0.85 Na (85% of apical membrane proton efflux is across the Na/H antiporter). Thus in the steady state, peritubular acidification causes an increased rate of luminal fluid acidification, which is accompanied by increased Na entry. Cell Na rises until the 3Na/2K-ATPase is stimulated sufficiently. The reverse happens with peritubular alkalinization. This biphasic time course in cell [Na] after peritubular acidification agrees with the results of Yoshitomi et al. (1985). These authors found that peritubular acidification caused cell Na activity to decrease by ~2 meq/liter in less than 5 s, and then to increase above control values over the next 10 s (Yoshitomi et al., 1985).

Changes in luminal pH lead to predictable changes in cell [Na]. Acidifying the lumen lowers cell [Na] and alkalinizing raises cell [Na]. Even with these experiments, the effect on cell [Na] is biphasic due to late effects of cell pH on the basolateral membrane $Na/3HCO_3$ cotransporter.

Fig. 10 *B* shows the effect of changing extracellular [Na] on cell [Na]. Interestingly, when peritubular [Na] is decreased to zero, cell [Na] decreases transiently and then increases to values above control levels. This finding is once again related to greater cell Na entry on the stimulated apical Na/H antiporter than Na loss on the basolateral $Na/3HCO_3$ cotransporter. The model predicts that luminal or luminal and peritubular Na removal profoundly lower cell Na concentration.

These findings disagree with the results of Yoshitomi and Fromter (1985). These authors found that peritubular and luminal Na removal each lowered cell Na concentration halfway toward zero. It is possible that this discrepancy is present because the model does not include basolateral membrane Na transporters other than those coupled to HCO_3. For instance, Fromter (1979) has reported the presence of Na-coupled aspartate and glutamate transporters on the basolateral membrane of the rat proximal tubule. However, aspartate and glutamate have not been present in the perfusates used experimentally, and there is no simple Na conductance on the basolateral membrane (Fromter, 1984). A more plausible explanation for this discrepancy involves changes in cell calcium concentration. It has been proposed that increases in intracellular calcium inhibit the apical membrane Na/H countertransporter (Lin et al., 1985). If so, then peritubular Na removal could raise cell calcium (basolateral Na/Ca exchange; Scoble et al., 1985) further lowering cell Na and preventing the late increase in cell Na concentration. The model does not contain such calcium-dependent regulatory mechanisms.

DISCUSSION

An electrokinetic model was developed to calculate transient changes in cell pH and ionic composition in the mammalian proximal tubule after perturbations in luminal or peritubular fluid composition. The general purposes of a model of this type are: (*a*) to analyze experimental findings quantitatively in terms of individual transporter rates; (*b*) to examine the physiological role of specific transporter characteristics (ion stoichiometry, allosteric regulation, saturability) in cell homeostasis; (*c*) to provide quantitative predictions for transport experiments; and (*d*) to serve as a basis upon which new experimental findings and hypotheses can be tested and incorporated. Similar models of epithelial transport have been reported for tight epithelia such as the urinary bladder (Lew et al., 1979; Civan and Bookman, 1982; Latta et al., 1984), and for the gallbladder, a leaky epithelium (Baerentsen et al., 1983).

The proximal tubule has been modelled previously using different mathematical approaches. Wang and Deen (1980) modelled steady-state HCO_3 resorption along the proximal tubule based on semi-empiric descriptions of the major tubule transporters. The model predicted radial and axial variations in CO_2 and HCO_3 concentrations and effects of carbonic anhydrase on transepithelial HCO_3 transport rates. Weinstein (1983) used non-equilibrium thermodynamic equations to describe steady-state volume, Na and acid flux across the proximal tubule. This was the first comprehensive model of the proximal tubule, which contained coupled ion transporters and the 3Na/2K-ATPase. The present work is an extension of the work of Weinstein focused specifically on predicting transient phenomena rather than steady-state cell solute concentrations. The present work contains newer information on the existence of the basolateral $Na/3HCO_3$ transporter and on the allosteric regulation of apical membrane Na/H countertransport. In addition, it was possible to include carrier saturabilities in our electrokinetic model, which were not used in the thermodynamic formulation.

Because of the complexity of the transport systems being described, it was necessary to choose a specific form for the equations relating transporter flux to the electrochemical driving force (Eq. 2). Similar equations were not required in previous epithelial transport models because multi-ion transporters having saturability and allosteric regulation were not encountered. The difficulty in developing appropriate transport equations is that the detailed kinetic mechanisms for most of the transporters are unknown. If the details of the transporters were defined, then a rigorous mathematical description of flux can be written (see Segal, 1975; Heinz, 1978). We have chosen a form for the generalized transport equation (Eq. 2), which satisfies both non-equilibrium thermodynamic and chemical kinetic requirements, and which can be applied when exact mechanistic data are not available. As discussed in the Model Formulation section, Eq. 2 reduces to standard equations in the limits of no substrate saturability, single ion transport, electroneutral transport, and zero substrate concentration on one side of the membrane. Although other generalized transport equations similar to Eq. 2 can be constructed, the calculated results are probably insensitive to the precise mathematical formulation used, particularly for calculations involving small perturbations from the steady state.

The model provides a good description of pH and Na regulation in the mammalian proximal tubule cell. Transporter permeabilities were selected exclusively from steady-state net transcellular fluxes; transporter affinities and allosteric dependencies were obtained from membrane vesicle and electrophysiologic studies. With minimal assumptions, the model predictions were in close agreement with both transient and steady-state electrophysiological and fluorescence measurements in the intact proximal tubule.

In addition to demonstrating that a model could be created that fit observed data, the model served two specific purposes. First, it allowed us to analyze how numerous apical and basolateral membrane transporters interact quantitatively to determine and regulate cell pH and Na. The model showed how luminal Na removal caused a biphasic response in cell pH (Alpern and Chambers, 1986), and why peritubular acidification caused a biphasic response in cell Na, an explanation that was not presented with the data of Yoshitomi et al. (1985).

In addition, the model made a number of predictions. In constructing the model, a small electroneutral K efflux pathway on the basolateral membrane was required to prevent cell K from rising continuously. This may represent the KCl cotransporter described by Eveloff et al. (1985). We also found that if the K basolateral conductance was not regulated allosterically by pH, cell depolarization secondary to peritubular acidification caused a massive K efflux.

The model also predicted that a significant apical membrane H-ATPase is present. Without such an ATPase, it was not possible to simulate the SITS-sensitive biphasic response to luminal Na removal (Alpern and Chambers, 1986). This finding agrees with recent findings from our laboratory where Preisig et al. (1986) examined the effect of luminal amiloride and more potent amiloride analogues on rates of HCO_3 absorption. They concluded that 65% of apical membrane proton secretion is mediated by the Na/H antiporter, while the remaining 35% is mediated by a different process, most likely an H-ATPase.

The model also demonstrated that the greater sensitivity of the cell to peritubular pH than to luminal pH could be attributed to the $Na/3HCO_3$ transporter without any allosteric regulation by pH (which was not present in the model). The high degree of pH sensitivity results in part from the third-power dependence of $Na/3HCO_3$ flux on HCO_3 concentration.

To focus on tubule acidification mechanisms without introducing uncertain parameters, all of the calculations performed were without initial osmotic gradients. Because cell volume changes were small (<10%) under these conditions, the assumption of fixed cell volume had little effect on the calculated results. To examine whether volume regulation is an intrinsic characteristic of the model, effects of imposed osmotic gradients on the time course of cell volume were determined. For both inwardly and outwardly directed gradients of a neutral impermeant solute (0–200 mM), there was rapid cell volume change (1–2 s, data not shown) without return of volume to its initial value. Therefore an additional dependence, as yet undefined, is required to explain volume regulatory phenomena. The model should prove to be useful in examining various theories of volume regulation.

The present model demonstrates that electrokinetic equations containing transporter saturability, allosteric dependences, and steady-state flux information can predict

transient changes in cell composition in response to perturbations in luminal or peritubular fluid composition. However, uncertainties remain in our understanding of proximal tubule function that prevent the model from being complete. As new data are obtained, these calculations can be modified to include Cl transport pathways, mechanisms of cell volume regulation, Ca regulatory mechanisms, and axial heterogeneity.

The authors gratefully acknowledge the continuing support and advice of Floyd C. Rector, Jr. The authors also acknowledge Alan Weinstein who offered helpful suggestions during the creation of the model.

These studies were supported by grants AM-35124 and AM-27045 from the National Institute of Arthritis, Diabetes, and Digestive and Kidney Diseases, U.C.S.F. grants from the Academic Senate, and the MSC Clough fund, a grant from the National Cystic Fibrosis Foundation, and by a generous grant from the Hedco Foundation. R. J. Alpern is the recipient of Clinical Investigator Award (AM-01229).

Received for publication 26 March 1986 and in final form 5 December 1986.

REFERENCES

Akiba, T., R. J. Alpern, J. Eveloff, J. Calamina, and D. G. Warnock. 1986. Electrogenic sodium/bicarbonate cotransport in rabbit renal cortical basolateral membrane vesicles. *J. Clin. Invest.* 78:1472–1478.

Alpern, R. J. 1984. Bicarbonate-water interactions in the rat proximal convoluted tubule: an effect of volume flux on active proton secretion. *J. Gen. Physiol.* 84:753–770.

Alpern, R. J. 1985. Mechanism of basolateral membrane $H^+/OH^-/HCO_3^-$ transport in the rat proximal convoluted tubule: a sodium-coupled electrogenic process. *J. Gen. Physiol.* 86:613–636.

Alpern, R. J., and M. Chambers. 1986. Cell pH in the rat proximal convoluted tubule: regulation by luminal and peritubular pH and sodium concentration. *J. Clin. Invest.* 78:501–510.

Alpern, R. J., M. G. Cogan, and F. C. Rector. 1982. Effect of luminal bicarbonate concentration on proximal acidification in the rat. *Am. J. Physiol.* 243:F53–F59.

Aronson, P. S., J. Nee, and M. A. Suhm. 1982. Modifier role of internal H^+ in activating the Na^+/H^+ exchanger in renal microvillus membrane vesicles. *Nature (Lond.).* 299:161–162.

Aronson, P. S., M. A. Suhm, and J. Nee. 1983. Interaction of external H^+ with the Na^+-H^+ exchanger in renal microvillus membrane vesicles. *J. Biol. Chem.* 258:6767–6771.

Bank, N., H. S. Aynedjian, and B. F. Mutz. 1985. Evidence for a DCCD-sensitive component of proximal bicarbonate absorption. *Am. J. Physiol.* 249:F636–F644.

Baerentsen, H., F. Giraldez, and T. Zeuthen. 1983. Influx mechanisms for Na^+ and Cl^- across the brush border membrane of leaky epithelia: a model and microelectrode study. *J. Membr. Biol.* 75:205–218.

Beck, F., R. Bauer, U. Bauer, J. Mason, A. Dorge, R. Rick, and K. Thurau. 1980. Electron microprobe analysis of intracellular elements in the rat kidney. *Kidney Int.* 17:756–763.

Biagi, B. A. 1985. Effects of the anion transport inhibitor, SITS, on the proximal straight tubule of the rabbit perfused in vitro. *J. Membr. Biol.* 88:25–31.

Biagi, B. A., and M. Sohtell. 1986. pH sensitivity of the basolateral membrane of the rabbit proximal tubule. *Am. J. Physiol.* 250:F261–F266.

Bomsztyk, K., and F. S. Wright. 1986. Dependence of ion fluxes on fluid transport by rat proximal tubule. *Am. J. Physiol.* 250:F680–F689.

Boron, W. F., and E. L. Boulpaep. 1983. Intracellular pH regulation in the renal proximal tubule of the salamander: basolateral HCO_3 transport. *J. Gen. Physiol.* 81:53–94.

Burckhardt, B.-Ch., A. C. Cassola, and E. Fromter. 1984*a*. Electrophysiological analysis of bicarbonate permeation across the peritubular cell membrane of the rat kidney proximal tubule. II. Exclusion of HCO_3^- effects on other ion permeabilities and of coupled electroneutral HCO_3^- transport. *Pfluegers Arch.*401:43–51.

Burckhardt, B.-Ch., K. Sato, and E. Fromter. 1984*b*. Electrophysiological analysis of bicarbonate permeation across the peritubular cell membrane of rat kidney proximal tubule. I. Basic observation. *Pfluegers Arch.* 401:34–42.

Cassola, A. C., M. Mollenhauer, and E. Fromter. 1983. The intracellular chloride concentration of rat kidney proximal tubular cells. *Pfluegers Arch.* 399:259–265.

Chan, Y.-L., and G. Giebisch. 1981. Relationship between sodium and bicarbonate transport in the rat proximal convoluted tubule. *Am. J. Physiol.* 240:F222–F230.

Civan, M. M., and R. J. Bookman. 1982. Transepithelial Na^+ transport and intracellular fluids: a computer study. *J. Membr. Biol.* 65:63–80.

Dwight, H. B. 1961. Tables of Integrals and Other Mathematical Data. 4th ed. Macmillan Publishing Co., New York. 132.

Edelman, A., S. Curci, I. Samarzija, and E. Fromter. 1978. Determination of intracellular K^+ activity in rat kidney proximal tubular cells. *Pfluegers Arch.* 378:37–45.

Eveloff, J., J. Calamia, and D. G. Warnock. 1985. KCl cotransport in rabbit renal cortical basolateral membrane vesicles. *Kidney Int.* 27:307. (Abstr.)

Fromter, E. K. 1977. Magnitude and significance of the paracellular shunt path in the kidney proximal tubule. *Excerpta Med. Int. Congr. Ser.* 391:393–405.

Fromter, E. 1979. Solute transport across epithelia: what can we learn from micropuncture studies on kidney tubules? *J. Physiol. (Lond.).* 288:1–31.

Fromter, E. 1982. Electrophysiological analysis of rat renal sugar and amino acid transport. I. Basic phenomena. *Pfluegers Arch.* 393:179–189.

Fromter, E. 1984. Viewing the kidney through microelectrodes. *Am. J. Physiol.* 247:F695–F705.

Fromter, E., G. Rumrich, and K. J. Ullrich. 1973. Phenomenologic description of Na^+, Cl^- and HCO_3^- absorption from proximal tubules of the rat kidney. *Pfluegers Arch.* 343:189–220.

Grassl, S. M., and P. S. Aronson. 1986. Na-HCO_3 cotransport in rabbit renal cortical basolateral membrane vesicles (BLMV). *Kidney Int.* 29:367 (Abstr.)

Guggino, W. B., E. L. Boulpaep, and G. Giebisch. 1982. Electrical properties of chloride transport across the Necturus proximal tubule. *J. Membr. Biol.* 65:185–196.

Guggino, W. B., R. London, E. L. Boulpaep, and G. Giebisch. 1983. Chloride transport across the basolateral cell membrane of the Necturus proximal tubule: dependence on bicarbonate and sodium. *J. Membr. Biol.* 71:227–240.

Heinz, E. 1978. Mechanics and energetics of biological transport. Springer-Verlag Publishers, New York. 63–120.

Hopfer, U., and R. Groseclose. 1980. The mechanism of Na^+-dependent D-glucose transport. *J. Biol. Chem.* 255:4453–4462.

Howlin, K. J., R. J. Alpern, and F. C. Rector, Jr. 1985. Amiloride inhibition of proximal tubular acidification. *Am. J. Physiol.* 248:F773–F778.

Illsley, N. P., P.-Y. Chen, and A. S. Verkman. 1986. Renal vesicle chloride transport measured by a novel chloride-sensitive fluorescent indicator. *Kidney Int.* 31:437. (Abstr.)

Jentsch, T. J., S. K. Keller, M. Koch, and M. Wiederhold. 1984. Evidence for coupled transport of bicarbonate and sodium in cultured bovine corneal endothelial cells. *J. Membr. Biol.* 81:189–204.

Jorgensen, P. L. 1980. Sodium and potassium ion pump in kidney tubules. *Physiol. Rev.* 60:864–917.

Kawahara, K. 1985. Ba^{2+}-sensitive potassium permeability of the apical membrane in newt kidney proximal tubule. *J. Membr. Biol.* 88:283–292.

Kinne-Saffran, E. R. Beauwens, and R. Kinne. 1982. An ATP-driven proton pump in brush-border membranes from rat renal cortex. *J. Membr. Biol.* 64:67–76.

Lakshminarayanaiah, N. 1984. Equations of membrane biophysics. Academic Press, Inc. New York. 130–151.

Lapointe, J.-Y., R. Laprade, and J. Cardinal. 1986. Characterization of the apical membrane ionic permeability of the rabbit proximal convoluted tubule. *Am. J. Physiol.*250:F339–F347.

Latta, R., C. Clausen, and L. C. Moore. 1984. General method for the derivation and numerical solution of epithelial transport models. *J. Membr. Biol.* 82:67–82.

Lew, V. L., H. G. Ferreira, and T. Moura. 1979. The behaviour of transporting epithelial cells. I. Computer analysis of a basic model. *Proc. R. Soc. Lond. B Biol. Sci.* 206:53–83.

Lin, J. T., L. Y. Chiu, E. Heinz, and E. E. Windhager. 1985. Effects of Ca on transport process in rat renal brush border membranes. *Kidney Int.* 27:315. (Abstr.)

Lucci, M. S., L. R. Pucacco, N. W. Carter, and T. D. DuBose, Jr. 1982. Direct evaluation of the permeability of the rat proximal convoluted tubule to CO_2. *Am. J. Physiol.* 242:F470–F476.

Meyer, M. M., and A. S. Verkman. 1987. Evidence for water channels in renal proximal tubule cell membranes. *J. Membr. Biol.* In press.

Preisig, P. A., H. E. Ives, E. J. Cragoe, R. J. Alpern, and F. C. Rector. 1987. The role of the Na^+/H^+ antiporter in rat proximal tubule bicarbonate absorption. *J. Clin. Invest.* In press.

Sasaki, S., K. Tomita, Y. Iino, T. Shiigai, and J. Takeuchi. 1986. Mechanism of bicarbonate exit across the basolateral membrane of rabbit proximal tubule. *Kidney Int.* 29:375. (Abstr.)

Schwartz, G. J., and Q. Al-Awqati. 1985. Carbon dioxide causes exocytosis of vesicles containing H^+ pumps in isolated perfused proximal and collecting tubules. *J. Clin. Invest.* 75:1638–1644.

Schwartz, G. J., A. M. Weinstein, R. E. Steele, J. L. Stephenson, and M. B. Burg. 1981. Carbon dioxide permeability of rabbit proximal convoluted tubules. *Am. J. Physiol.* 249:F231–F244.

Scoble, J. E., S. Mills, and K. A. Hruska. 1985. Calcium transport in canine renal basolateral membrane vesicles: effects of parathyroid hormone. *J. Clin. Invest.* 75:1096–1105.

Segel, I. H. 1975. Enzyme Kinetics. Behavior and Analysis of Rapid Equilibrium and Steady-state Enzyme Systems. John Wiley & Sons, Inc., New York. 847–884.

Shindo, T., and K. R. Spring. 1981. Chloride movement across the basolateral membrane of proximal tubule cells. *J. Membr. Biol.* 58:35–42.

Strickholm, A., and B. G. Wallin. 1967. Relative ion permeabilities in the crayfish giant axon determined from rapid external ion changes. *J. Gen. Physiol.* 50:1929–1953.

Thurau, K., A. Dorge, J. Mason, F. Beck, and R. Rick. 1979. Intracellular elemental concentrations in renal tubular cells. An electron microprobe analysis. *Klin. Wochenschr.* 57:993–999.

Verkman, A. S., J. A. Dix, and J. L. Seifter. 1985. Water and urea transport in renal microvillus membrane vesicles. *Am. J. Physiol.* 248:F650–F655.

Verkman, A. S., and H. E. Ives. 1986*a*. Anomalous driving force for renal brush border H^+/OH^- transport characterized using 6-carboxyfluorescein. *Biochemistry.* 25:2876–2882.

Verkman, A. S., and H. E. Ives. 1986*b*. Water transport and fluidity in renal basolateral membranes. *Am. J. Physiol.* 250:F633–F643.

Verkman. A. S. 1987. Passive H^+/OH^- permeability in epithelial brush border membranes. *J. Bioenerg. Biomembr.* In press.

Wang, K. W., and W. M. Deen. 1980. Chemical kinetic and diffusional limitations on bicarbonate reabsorption by the proximal tubule. *Biophys. J.* 31:161–182.

Warnock, D. G., and J. Eveloff. 1982. NaCl entry mechanisms in the luminal membrane of the renal tubule. *Am. J. Physiol.* 242:F561–F574.

Wasserstein, A. G., and Z. S. Agus. 1983. Potassium secretion in the rabbit proximal straight tubule. *Am. J. Physiol.* 245:F167–F174.

Weinstein, A. M. 1983. Nonequilibrium thermodynamic model of the rat proximal tubule epithelium. *Biophys. J.* 44:153–170.

Yoshitomi, K., B.-Ch. Burckhardt, and E. Fromter. 1985. Rheogenic sodium-bicarbonate cotransport in the peritubular cell membrane of rat renal proximal tubule. *Pfluegers Arch.* 405:360–366.

Yoshitomi, K., and E. Fromter. 1984. Cell pH of rat renal proximal tubule in vivo and the conductive nature of peritubular HCO_3^- (OH^-) exit. *Pfluegers Arch.* 402:300–305.

Yoshitomi, K., and E. Fromter. 1985. How big is the electrochemical potential difference of Na^+ across rat renal proximal tubular cell membranes in vivo? *Pfluegers Arch.* 405 (suppl)1:5121–5126.

Young, D. M., and R. T. Gregory. 1973. A Survey of Numerical Mathematics. Vol. I. Addison-Wesley Publishing Co. Inc., Reading, MA. 164–166.